

Research Paper

Human parthenogenetic neural stem cell grafts promote multiple regenerative processes in a traumatic brain injury model

Jea-Young Lee¹, Sandra Acosta¹, Julian P. Tuazon¹, Kaya Xu¹, Hung Nguyen¹, Trenton Lippert¹, Michael G. Liska¹, Andrey Semechkin², Ibon Garitaonandia², Rodolfo Gonzalez², Russell Kern^{2,3}, Cesario V. Borlongan^{1,✉}

1. Center of Excellence for Aging and Brain Repair, Department of Neurosurgery and Brain Repair, USF Morsani College of Medicine, Tampa, FL.
2. International Stem Cell Corporation, Carlsbad, CA.
3. Cyto Therapeutics, Melbourne, Australia.

✉ Corresponding author: Cesario V. Borlongan, PhD. Tel: 813-974-3988; Fax: 813-974-3078; Email: cborlong@health.usf.edu

© Ivyspring International Publisher. This is an open access article distributed under the terms of the Creative Commons Attribution (CC BY-NC) license (<https://creativecommons.org/licenses/by-nc/4.0/>). See <http://ivyspring.com/terms> for full terms and conditions.

Received: 2018.09.11; Accepted: 2018.11.16; Published: 2019.01.30

Abstract

International Stem Cell Corporation human parthenogenetic neural stem cells (ISC-hpNSC) have potential therapeutic value for patients suffering from traumatic brain injury (TBI). Here, we demonstrate the behavioral and histological effects of transplanting ISC-hpNSC intracerebrally in an animal model of TBI.

Methods: Sprague-Dawley rats underwent a moderate controlled cortical impact TBI surgery. Transplantation occurred at 72 h post-TBI with functional readouts of behavioral and histological deficits conducted during the subsequent 3-month period after TBI. We characterized locomotor, neurological, and cognitive performance at baseline (before TBI), then on days 0, 1, 7, 14, 30, 60, and 90 (locomotor and neurological), and on days 28-30, 58-60, and 88-90 (cognitive) after TBI. Following completion of behavioral testing at 3 months post-TBI, animals were euthanized by transcardial perfusion and brains harvested to histologically characterize the extent of brain damage. Neuronal survival was revealed by Nissl staining, and stem cell engraftment and host tissue repair mechanisms such as the anti-inflammatory response in peri-TBI lesion areas were examined by immunohistochemical analyses.

Results: We observed that TBI groups given high and moderate doses of ISC-hpNSC had an improved swing bias on an elevated body swing test for motor function, increased scores on forelimb akinesia and paw grasp neurological tests, and committed significantly fewer errors on a radial arm water maze test for cognition. Furthermore, histological analyses indicated that high and moderate doses of stem cells increased the expression of phenotypic markers related to the neural lineage and myelination and decreased reactive gliosis and inflammation in the brain, increased neuronal survival in the peri-impact area of the cortex, and decreased inflammation in the spleen at 90 days post-TBI.

Conclusion: These results provide evidence that high and moderate doses of ISC-hpNSC ameliorate TBI-associated histological alterations and motor, neurological, and cognitive deficits.

Key words: neuroprotection, traumatic brain injury, human parthenogenetic neural stem cells, inflammation, stem cell transplantation

Introduction

Traumatic brain injury (TBI) affects 1.4 million individuals each year and can lead to death or disability with motor, neurological, and cognitive impairments [1-3]. In the U.S., 30.5% of all injury-associated deaths involve TBI [4]. The disease is characterized by two phases of injury and the first

phase involves an initial head trauma via an external force that results in mechanical damage to brain tissue [1, 5, 6]. Afterwards, secondary biochemical cascades can lead to inflammation, apoptosis, oxidative stress, and other complications that promote additional injury and further exacerbate symptoms [6-8]. Thus, it

is imperative to target these secondary biochemical pathways to preclude additional brain damage [6, 8, 9].

Cell-based therapy may be a viable method of ameliorating the negative effects of TBI. Human pluripotent stem cells such as human parthenogenetic stem cells (hpSCs) are enticing because they are capable of limitless division, differentiation into all cell types, and a vast array of uses in medical treatments [10, 11]. An endless, expandable, and cryopreservable supply of homogenous International Stem Cell Corporation human parthenogenetic neural stem cells (ISC-hpNSC) can be created using chemically-induced differentiation [12-15]. Unlike human embryonic stem cells, ISC-hpNSC circumvent the ethical dilemma of using a potential human embryo because they are generated from chemically-activated unfertilized oocytes [13, 16, 17]. Additionally, hpSCs can facilitate easier derivation of homozygous human leukocyte antigen types to potentially immune match more patients and avoid graft rejection after transplantation [13, 18-20]. Concerns about clinical applications of stem cells include their safety and the potential tumorigenic properties of lingering, undifferentiated human pluripotent stem cells [10, 21, 22]. However, ISC-hpNSC have been grafted successfully, are tolerated well by animals, and have inconsequential tumorigenicity [10, 13, 23]. Previous studies have exhibited how stem cell transplantation improves various neurological diseases in pre-clinical animal models, including Parkinson's disease, TBI, stroke, Alzheimer's disease, and amyotrophic lateral sclerosis [13, 24-28]. Intravenous transplantation of human adipose-derived stem cells in animal TBI models provided neuroprotection and decreased cortical damage and neuronal loss in the hippocampus [27]. Moreover, ISC-hpNSC transplanted in the brains of Parkinson's disease animal models improved behavioral and histological deficits without detrimental effects such as tumor formation [13]. With these promising results, an alluring next step would be to examine the effects of ISC-hpNSC transplanted into a TBI brain model. In the present study, we evaluated the efficacy of ISC-hpNSC transplanted intracerebrally to ameliorate behavioral and histological deficits in controlled cortical impact TBI model rats.

Methods

Study subjects

Experimental procedures were approved by the University of South Florida Institutional Animal Care and Use Committee (IACUC). All studies were

conducted in accordance with the National Institutes of Health Guide for the Care and Use of Laboratory Animals and the United States Public Health Service's Policy on Humane Care and Use of Laboratory Animals. All animals were housed under normal conditions (20 °C, 50% relative humidity, and a 12 h light/dark cycle). A total of 70 adult male Sprague-Dawley rats (two months-old, 250-300 g) were used. Only animals identified at baseline (prior to TBI surgery) as exhibiting normal behaviors (elevated body swing test (EBST): 50-60% swing bias; rotarod test: lasting 60 s on rotating rod; Bederson neurological exam: at least 0-0.5 mean neurologic score) received TBI or sham surgery. Moreover, only TBI animals reaching the criterion of behavioral impairment (EBST: at least 75% swing bias; rotarod test: lasting 30 s or less on rotating rod; Bederson neurological exam: at least 2.5 mean neurologic score) were arbitrarily assigned to the following groups: vehicle-only, low dose of ISC-hpNSC, moderate dose of ISC-hpNSC, or high dose of ISC-hpNSC. Each experimental group consisted of $n = 12$ subjects.

TBI surgery

Animals were subjected to either TBI using a controlled cortical impact (CCI) injury model or sham control (no TBI). All surgical procedures were conducted under aseptic conditions. The animals were anesthetized with 1.5% isoflurane and checked for pain reflexes. Under deep anesthesia, animals underwent the moderate TBI model. Each animal was placed in a stereotaxic frame and anesthesia maintained via gas mask with 1-2% isoflurane. After exposing the skull, a 4-mm craniectomy was performed over the left frontoparietal cortex (center at -2.0 mm AP and +2.0 mm ML to bregma). A pneumatically operated metal impactor (diameter = 3 mm) impacted the brain at a velocity of 6.0 m/s, reaching a depth of 1.0 mm below the dura mater layer, and remained in the brain for 150 ms. The impactor rod was angled 15° to the vertical to be perpendicular to the tangential plane of the brain curvature at the impact surface. A linear variable displacement transducer (Macrosensors, Pennsauken, NJ) connected to the impactor measured velocity and duration to ensure consistency. After CCI injury, the incision was sutured after bleeding ceased. An integrated heating pad and rectal thermometer unit with feedback control allowed maintenance of body temperature at normal limits. All animals were monitored until recovery from anesthesia. In addition, animals were weighed and observed daily for the next 3 consecutive days following TBI surgery, weighed twice a week thereafter, and monitored daily for health status and any signs that indicated problems or

complications throughout the study. For a general documentation of behavioral status of the animals, video clips were made at baseline, post-TBI and post-transplant time points.

Grafting procedures

All surgical procedures were conducted under aseptic conditions. Animals were anesthetized with 1.5% isoflurane. Once deep anesthesia was achieved (by checking for pain reflexes), hair was shaved around the area of surgical incision (skull area) with enough border to prevent contamination of the operative site, followed by two surgical germicidal scrubs of the site, and draping with sterile drapes. The animal was fixed to a Stereotaxic apparatus (Kopf Instruments) and a 26-gauge Hamilton syringe was then lowered into a small burred skull opening. The syringe needle was inserted twice to administer ISC-hpNSC over two deposits, which were performed in two target brain areas: the cortex (AP = 0.5 mm; ML = 1 mm; DV = 2.0 mm), which represents the peri-TBI area, and the hippocampus (AP = -5 mm; ML = 4.5 mm; DV = 4.5 mm), a brain structure remote from the primary injured cortex that exhibits secondary cell death processes [29]. With each deposit, either 50,000 cells for the low dose, 100,000 cells for the moderate dose, or 200,000 cells for the high dose, each in 3 μ L volumes, were infused over a period of 3 min. Thus, a total of 100,000 cells for the low dose, 200,000 cells for the moderate dose, and 400,000 cells for the high dose, each in a total of 6 μ L volumes, were delivered over the two deposits. Following an additional 2-min absorption time, the needle was retracted and the wound closed with a stainless steel wound clip. A heating pad and a rectal thermometer allowed maintenance of body temperature at about 37 °C throughout surgery and following recovery from anesthesia.

ISC-hpNSC

ISC-hpNSC were manufactured as in our previous study [10]. The LLC2P hpSC line (ISCO) was maintained on human neonatal skin fibroblasts (ISCO), underwent mechanical passaging, was cultured under current good manufacturing practice conditions in Knockout DMEM/F12 (Life Technologies), and was supplemented with 0.1 mM beta-mercaptoethanol (Life Technologies), 2 mM GlutaMAX (Invitrogen), 15% Knockout Serum Replacement (Life Technologies), 5 ng/mL basic fibroblast growth factor (Thermo Fisher Scientific), and 0.1 mM Minimum Essential Medium nonessential amino acids (Life Technologies). Prior to neural induction and under feeder-free and xeno-free conditions, cells were passaged three times in Essential 8 Medium (Thermo Fisher Scientific) on Cell

Therapy Systems CELLStart substrate (Thermo Fisher Scientific) and subcultured with StemPro Accutase (Thermo Fisher Scientific). Upon 80% confluency, cells were neuralized for 11 days by adding 1 μ M DMH-1 (Tocris) and 5 μ M SB218078 (Tocris), and placed in 1 \times GlutaMAX (Invitrogen), 1 \times N2/B27 Supplement (Thermo Fisher Scientific), and Knockout DMEM/F12 (Life Technologies). After dissociation with Y-27632 dihydrochloride (Tocris) and StemPro Accutase (Thermo Fisher Scientific), neuralized cells were then plated on Cell Therapy Systems CELLstart-coated dishes (Thermo Fisher Scientific) in StemPro NSC Serum Free Medium (Thermo Fisher Scientific). Cell banks were created by expanding and cryopreserving ISC-hpNSC and were tested for pluripotency and neural markers.

Behavioral and neurological tests

All investigators testing the animals were blinded to the treatment condition. Each rat was subjected to a series of behavioral tests to reveal motor, neurological, and cognitive performances of animals before and after TBI and after transplantation. The tests included the elevated body swing test (EBST), Bederson neurological exam, rotarod test, and radial arm water maze test (RAWM). The EBST and the neurological exam were conducted at baseline, on day 0 (day of TBI surgery), and on days 1, 7, 14, 30, 60, and 90 after TBI. The rotarod test was performed on days 7, 14, 30, 60, and 90 post-TBI. RAWM sessions were executed on days 28-30, 58-60, and 88-90 following TBI (Figure 1A).

Elevated body swing test (EBST)

EBST involved handling the animal by its tail and recording the direction of the swings. The test apparatus consisted of a clear Plexiglas box (40 \times 40 \times 35.5 cm). The animal was gently picked up at the base of the tail and elevated by the tail until the animal's nose was at a height of 2 inches (5 cm) above the surface. The direction of the swing, either left or right, was counted once the animal's head moved sideways approximately 10° from the midline position of the body. After a single swing, the animal was placed back in the Plexiglas box and allowed to move freely for 30 s prior to retesting. These steps were repeated 20 times for each animal. Normally, intact rats display a 50% swing bias, that is, the same number of swings to the left and to the right. A 75% swing bias would indicate 15 swings in one direction and 5 in the other during 20 trials. We have previously utilized the EBST and noted that lesioned animals display >75% biased swing activity at one month after a nigrostriatal lesion; asymmetry was stable for up to six months [30].

Modified Bederson neurological exam

About one hour after the EBST, a modified Bederson neurological exam was conducted following the procedures previously described [31] with minor modifications. Neurologic score for each rat was obtained using two tests that included forelimb akinesia, which measured the ability of the animal to replace the forelimb after it was displaced laterally by 2-3 cm, graded from 0 (immediate replacement) to 3 (replacement after several seconds or no replacement), and bilateral forepaw grasp, which measured the ability to hold onto a 2 mm-diameter steel rod, graded 0 for a rat with normal forepaw grasping behavior to 3 for a rat unable to grasp with the forepaws.

Rotarod test

An hour after completion of the neurological exam, the animals were then subjected to the rotarod test. The rotarod test involved placement of the animal on an accelerating rotarod (Accuscan, Inc.) that used a rotating treadmill that accelerated from 4 rpm to 40 rpm over a 5-min period. The total number of seconds maintained on the rotarod was recorded and used as an index of motor coordination. We have previously shown that TBI model animals exhibited significantly shorter times on the rotarod compared to sham operated or normal controls.

Radial arm water maze (RAWM) test

To reveal the cognitive effects of hpNSC grafts on spatial navigation and memory of young and aged TBI rats, RAWM, a hippocampal-dependent task, was employed. RAWM was performed on day 30, day 60, and day 90 after TBI surgery and intracerebral transplantation of hpNSC grafts or vehicle. Six-arm RAWM were placed in an ~150 cm-diameter water tank and a 40 cm-tall, 10 cm-diameter platform was used. The platform was submerged 1 cm below the surface of the water. The temperature of the water was kept at 27 °C. Rats were placed on the start arm at the beginning of every trial, and the platform was located on the goal arm. Every animal had an assigned platform/arm location throughout acquisition of learning, yet the starting zone was randomly changed each trial. A space-training protocol was followed. Rats were given two blocks of four trials, with each block separated by a 30 min rest period, for a total of eight trials each day for 3 days of acquisition of learning. Trials were only 60 s long. Once animals found their goal arm/platform, they were allowed to remain on the platform for 30 s between trials. If rats were unable to find their goal arm/platform within 60 s, rats were guided to their goal arm and allowed to rest on the platform for 30 s.

On day 4, a probe trial was given 1 h before reversal training started, placing the rat 180° from the goal arm. Rats were given four trials to train for the new position (reversal training). RAWM performance analysis was done by averaging the trials per block, using four trials per block and then a total of two blocks per day (errors were given every time rats did not enter the goal arm). Reversal training was analyzed by counting the total of errors in each trial.

Perfusion

Brain section preparation was designed to identify the extent of brain damage and host cell survival. A small cohort of animals ($n = 10$) that received the same TBI and ISC-hpNSC transplantation procedures were euthanized at 17 days after TBI to reveal early graft survival via labeling with the human specific neural cell adhesion molecule (NCAM) antibody (**Figure 1B**). At the scheduled post-transplantation period (3 months) after TBI, rats were randomly euthanized and perfused by transcardial perfusion with 4% paraformaldehyde. The brains and spleens were dissected, post-fixed overnight in 4% paraformaldehyde, then subsequently immersed in 30% sucrose. Each spleen was cut into 40 µm-thick coronal tissue sections and each forebrain was cut into 40 µm-thick coronal tissue sections with anterior-posterior coordinates corresponding from bregma 5.2 mm to bregma -8.8 mm [29].

Nissl staining

Nissl staining was performed with 0.1% cresyl violet solution (Sigma-Aldrich) using a standard protocol to evaluate the peri-impact injury of our TBI model [26, 27]. From each perfused brain, six coronal sections between the anterior edge and posterior edge of the TBI impact area were collected and processed for Nissl staining. The peri-impact area was defined as the region in the cortex immediately surrounding the TBI impact area, starting at AP +2.0 mm and ending at AP -3.8 mm posterior from the bregma. Every sixth coronal tissue section was chosen at random to quantify cell survival in the peri-impact area. Brain sections were examined using a light microscope (Keyence). Neuronal survival in the peri-impact area of the brain was quantified using a computer-assisted image analysis system (NIH Image Software, USA) and was expressed as a percentage of the ipsilateral hemisphere compared to the contralateral hemisphere [27].

Immunohistochemistry protocol

The cell engraftment index for human neural stem cell graft survival was assessed using monoclonal human specific antibody HuNu and other

human specific antibodies that do not cross-react with rodent proteins. Additional brain and spleen sections were processed for mechanism-based immunohistochemical analyses of tissue samples focusing on inflammation. Immunofluorescence labeling was conducted on every third coronal section of the brain and every sixth coronal section of the spleen. Briefly, sections were washed three times for 10 min in 0.1 M tris buffer solution (TBS). Six sections were incubated with saline sodium citrate (SSC) solution at pH 6.0 for 40 min at 80 °C for antigen retrieval purposes. Then, samples were blocked for 60 min at room temperature with 8% normal goat serum (Invitrogen, CA) in 0.1 M TBS containing 0.1% Tween 20 (TBST) (Sigma). Sections were then incubated overnight at 4 °C with corresponding primary antibody with 10% normal goat serum. The primary antibodies used for brain tissue were goat monoclonal anti-major histocompatibility complex class II (MHCII; 1:750; BD; 554926), rabbit polyclonal anti-tumor necrosis factor (TNF; 1:200; Novus; 19532), mouse monoclonal anti-neural cell adhesion molecule (NCAM; 1:500; Abcam; ab200698), rabbit polyclonal anti-SOX1 (SOX1; 1:500; Abcam; ab87775), mouse monoclonal anti-human nuclei (HuNu; 1:50; Millipore; MAB1281), rabbit polyclonal anti-gial fibrillary acidic protein (GFAP; 1:250; Abcam; ab7260), rabbit polyclonal anti-nestin (1:100; Abcam; ab92391), rabbit polyclonal anti-microtubule-associated protein 2 (MAP2; 1:100, Abcam; ab32454), rabbit polyclonal anti-myelin basic protein (MBP; 1:200, Abcam; ab40390), and goat anti-doublecortin (DCX; 1:150; Santa Cruz; sc-8066). The primary antibodies used for

spleen tissue were anti-major histocompatibility complex class II (MHCII; 1:750 BD; 554926) and rabbit polyclonal anti-tumor necrosis factor (TNF; 1:200; Novus; 19532). Then, sections were washed five times for 10 min in 0.1 M TBST and soaked in 5% normal goat serum in 0.1 M TBST containing corresponding secondary antibodies, goat anti-mouse IgG-Alexa 488 (green) (1:400; Invitrogen) or goat anti-rabbit IgG-Alexa 594 (red) (1:2000; Invitrogen) for 90 min. Finally, coronal sections were washed five times for 10 min in 0.1 M TBST and three times for 5 min in 0.1 M TBS, processed for 1:300 Hoechst 33258 (bisBenzimideH 33258 trihydrochloride, Sigma) for 30 min, washed in 0.1 M TBS, and cover-slipped with Fluoromount (Aqueous Mounting Medium; Sigma; F4680). Coronal sections were examined using a confocal microscope (Zeiss). Control studies included exclusion of primary antibody substituted with 5% normal goat serum in 0.1 M TBS. No immunoreactivity was observed in these controls.

Immunohistochemistry data and immunofluorescence average labeling intensity analysis

Randomly selected high-power fields corresponding to the peri-impact region were used to count surviving grafted cells and inflammatory cells in this region. Briefly, 40 µm cryostat-sectioned tissues were examined at 4× magnification and digitized using Axio Vision (Zeiss) and BZ-II Analyzer (Keyence). Brain sections were blind-coded and Abercrombie's formula was used to calculate the total number of immunopositive cells [32, 33].

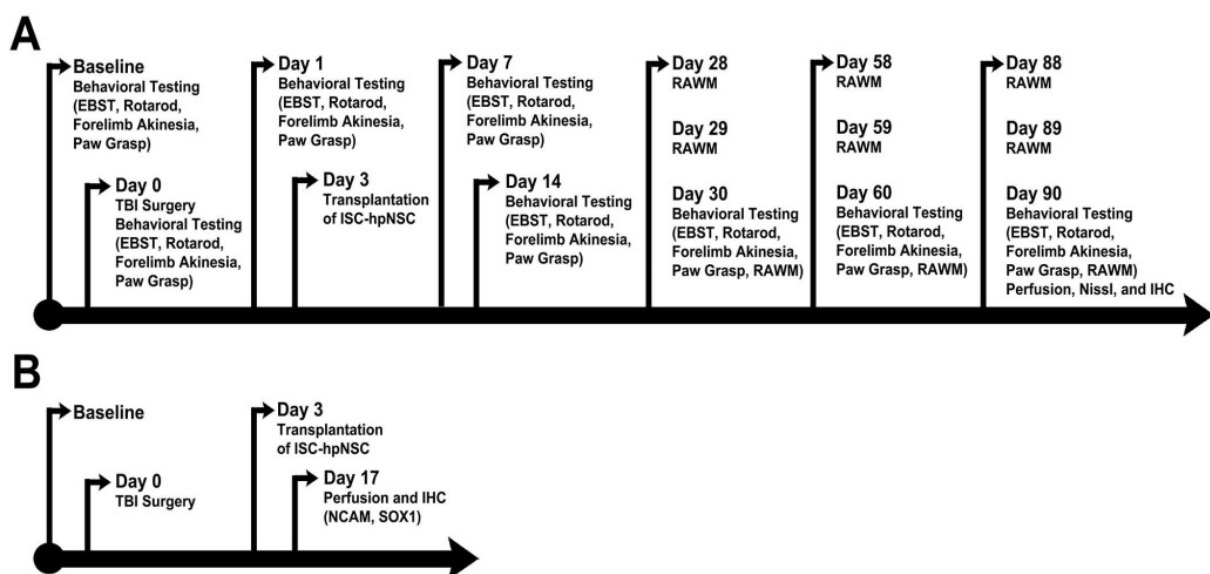


Figure 1. Timelines of experimental protocols. (A) Long-term survival timeline. **(B)** Short-term survival timeline. Animals were perfused on day 17 after TBI to assess short-term ISC-hpNSC graft survival. EBST: elevated body swing test; RAWM: radial arm water maze test; IHC: immunohistochemistry; NCAM: neural cell adhesion molecule; ISC-hpNSC: International Stem Cell Corporation human parthenogenetic neural stem cells.

For each labeling treatment, six coronal sections of the brain and eight coronal sections of the spleen were collected from each animal. From each section, approximately 4 to 6 images at 20 \times magnification were taken using a confocal microscope (Zeiss) and analyzed with ImageJ (National Institutes of Health, Bethesda, MD). All photomicrographs were converted to gray scale. Background was selected from blank control images and subsequently used to subtract the background from all images. The same threshold was used for all images. Thereafter, the labeling intensity of each section was quantified as the average optical density readings of 4 to 6 randomly selected areas within that section. The final labeling intensity of each group was expressed as the average of each labeling intensity per section.

Statistical analysis

The data were evaluated statistically using one-way analysis of variance (ANOVA) and subsequent post hoc Bonferroni's test for behavior. Statistical significance was preset at $p < 0.05$. (GraphPad version 5.01). The Kolmogorov-Smirnov test was performed to assess normality and the resulting values were less than 5% of the critical values.

Results

ISC-hpNSC improve behavioral performance in TBI animals

We performed an elevated body swing test (EBST) to evaluate locomotor performance after TBI and after ISC-hpNSC transplantation in TBI rats. All TBI animals initially showed a strong swing bias on day 0 (**Figure 2A**). However, by day 7 and onwards, high-dose and moderate-dose groups exhibited a significantly improved swing bias ($p < 0.05$) relative to vehicle and low-dose groups (**Figure 2A**). Afterwards, rotarod tests measured TBI rats' motor coordination post-TBI and post-transplantation. On day 7 and beyond, all TBI groups experienced considerably shorter times on the rod compared to the sham-control group and had similar test results (**Figure 2B**). Analysis of variance (ANOVA) revealed no significant treatment effects ($p > 0.05$). Next, a modified Bederson neurological exam assessed neurological function in animal subjects. Similar to the EBST, TBI groups demonstrated impaired scores on day 0 of the forelimb akinesia and paw grasp tests relative to baseline scores (**Figure 2C-D**). On day 14 and after, all TBI groups transplanted with stem cells displayed significantly lower scores ($p < 0.05$) than the

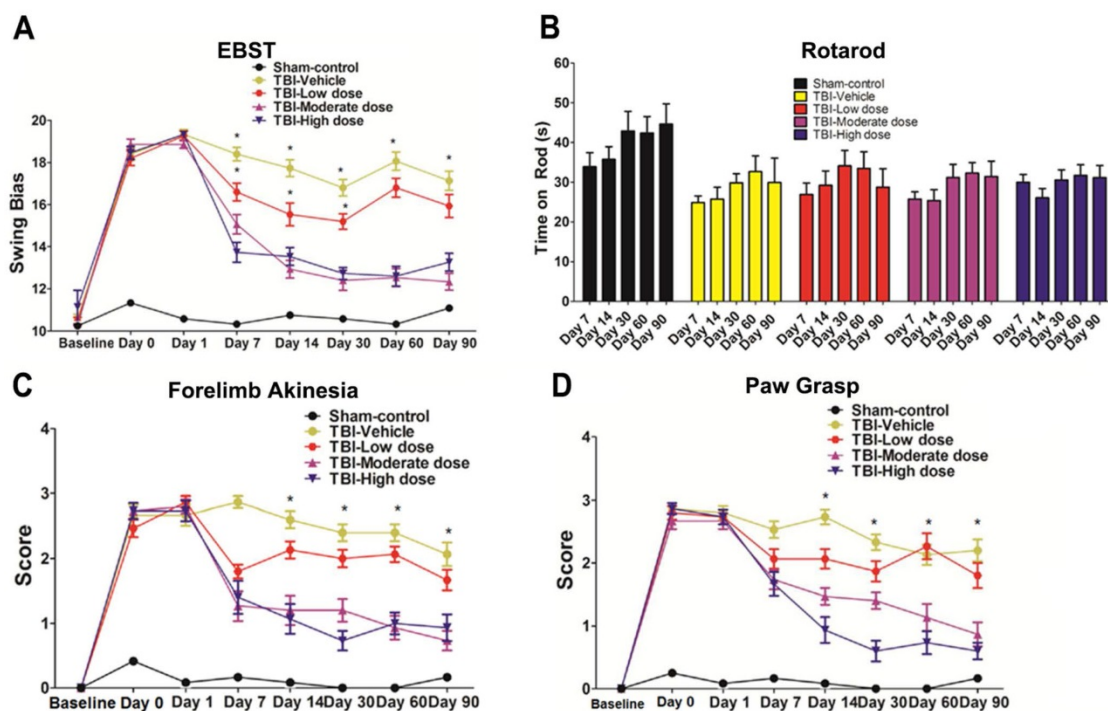


Figure 2. Behavioral tests to evaluate motor and neurological performance. The Kolmogorov-Smirnov test was performed to assess normality and resulting values were less than 5% of the critical values. $n = 12$ animals for each group. **(A)** Locomotor assessment as evaluated by elevated body swing test (EBST). Results were analyzed using one-way ANOVA for each time point ($*p < 0.05$). Statistical analysis: ANOVA revealed significant treatment effects (EBST, $F(4,67) = 9.54$, $p < 0.0001$, Bonferroni's test $p < 0.05$). **(B)** Motor coordination as revealed by rotarod test. Results were analyzed using one-way ANOVA for each time point. Statistical analysis: ANOVA revealed no significant treatment effects ($p > 0.05$). **(C)** Neurological assessment as evaluated by forelimb akinesia test. Results were analyzed using one-way ANOVA for each time point ($*p < 0.05$). Statistical analysis: ANOVA revealed significant treatment effects (FL, $F(4,67) = 9.885$, $p < 0.0001$, Bonferroni's test $p < 0.05$). **(D)** Neurological assessment as evaluated by paw grasp test. Results were analyzed using one-way ANOVA for each time point ($*p < 0.05$). Statistical analysis: ANOVA revealed significant treatment effects (PG, $F(4,67) = 10.42$, $p < 0.0001$, Bonferroni's test $p < 0.05$).

vehicle group on the forelimb akinesia and paw grasp tests, especially groups given high and moderate doses (Figure 2C-D). We then executed the radial arm water maze (RAWM) test to analyze cognitive performance following TBI and transplantation. All groups committed progressively fewer errors as they completed more trials in a day. There were significant differences between the vehicle group and each of the

stem cell treatment groups ($p < 0.05$). Additionally, high-dose and moderate-dose groups had significantly fewer errors ($p < 0.05$) than low-dose groups (Figure 3A-C). Moreover, no significant difference was found ($p > 0.05$) between moderate-dose and high-dose groups for all probe trials (Figure 3A-C).

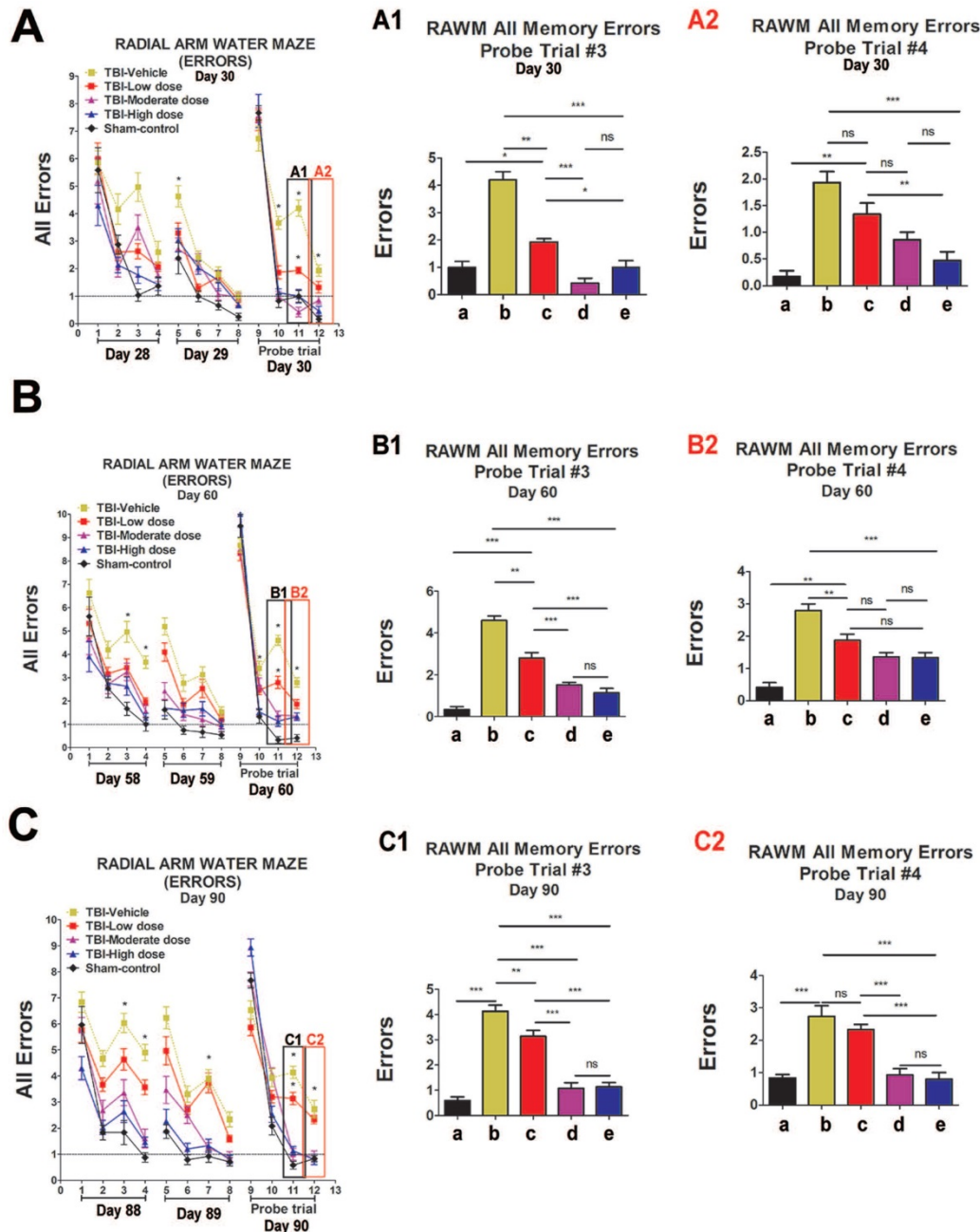


Figure 3. Cognitive effects of ISC-hpNSC on spatial navigation and memory as measured by errors made on radial arm water maze test (RAWM). Four blocks were performed per day, with each block consisting of two trials. Results were analyzed using one-way ANOVA for each time point ($*p < 0.05$; $**p < 0.001$; $***p < 0.0001$; ns $p > 0.05$). The Kolmogorov-Smirnov test was performed to assess normality and resulting values were less than 5% of the critical values. $n = 12$ animals for each group. A1: day 30, probe trial 3; A2: day 30, probe trial 4; B1: day 60, probe trial 3; B2: day 60, probe trial 4; C1: day 90, probe trial 3; C2: day 90, probe trial 4. a: Sham-Control; b: TBI-Vehicle; c: TBI-Low dose; d: TBI-Moderate dose; e: TBI-High dose. (A) Day 30 post-TBI, probe trial 3. Statistical analysis: ANOVA revealed significant treatment effects (RAWM, $F(4,67)=43.55$, $p < 0.0001$, Bonferonni's test $p < 0.05$). Day 30 post-TBI, probe trial 4. Statistical analysis: ANOVA revealed significant treatment effects (RAWM, $F(4,67)=43.55$, $p < 0.0001$, Bonferonni's test $p < 0.05$). (B) Day 60 post-TBI, probe trial 3. Statistical analysis: ANOVA revealed significant treatment effects (RAWM, $F(4,67)=18.97$, $p < 0.0001$, Bonferonni's test $p < 0.05$). Day 60 post-TBI, probe trial 4. Statistical analysis: ANOVA revealed significant treatment effects (RAWM, $F(4,67)=18.97$, $p < 0.0001$, Bonferonni's test $p < 0.05$). (C) Day 90 post-TBI, probe trial 3. Statistical analysis: ANOVA revealed significant treatment effects (RAWM, $F(4,67)=21.27$, $p < 0.0001$, Bonferonni's test $p < 0.05$). Day 90 post-TBI, probe trial 4. Statistical analysis: ANOVA revealed significant treatment effects (RAWM, $F(4,67)=21.27$, $p < 0.0001$, Bonferonni's test $p < 0.05$).

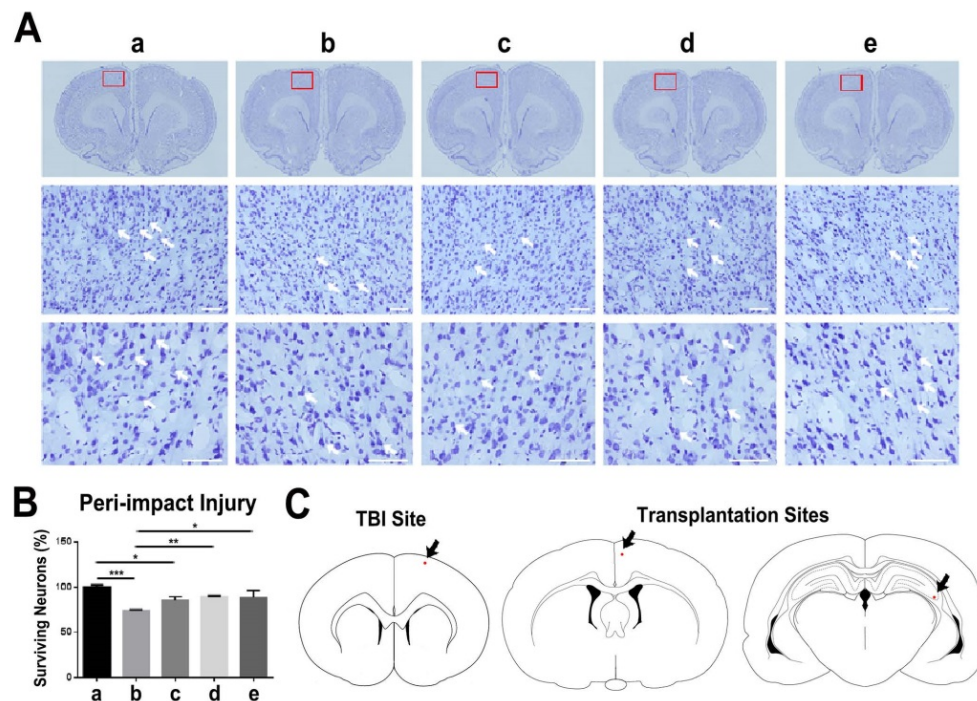


Figure 4. Assessment of neuronal survival in the peri-impact area and locations of TBI site and ISC-hpNSC transplantation sites. (A) Images of the peri-impact area in the cortex. Arrows indicate surviving cells. Scale bar = 50 μ m. **(B)** Quantitative analysis of neuronal survival. Statistical analysis: ANOVA revealed significant differences between vehicle and sham groups (*** $p < 0.001$), vehicle and moderate dose groups (** $p < 0.01$), vehicle and high dose groups (* $p < 0.05$), low dose and sham groups (* $p < 0.05$), and no significant differences between moderate dose and sham groups and between high dose and sham groups ($p > 0.05$). $n = 12$ animals for each group. The red box indicates the peri-impact area. **(A-B)** a: Sham-Control; b: TBI-Vehicle; c: TBI-Low dose; d: TBI-Moderate dose; e: TBI-High dose. **(C)** Representative diagrams identifying the location of the TBI site and ISC-hpNSC transplantation sites. Transplantation sites were located in the cortex and hippocampus regions. Red dots and arrows indicate the TBI site and ISC-hpNSC transplantation sites.

ISC-hpNSC attenuate histological deficits in the TBI brain

Nissl staining with 0.1% cresyl violet was performed to stain Nissl bodies in neurons and evaluate neuronal survival in the peri-impact area of the cortex. The TBI-vehicle and TBI-low dose groups had a percentage of neuronal survival that was significantly different from that of the sham group ($p < 0.001$; $p < 0.05$). Additionally, TBI-moderate dose and TBI-high dose groups had a significantly higher percentage of neuronal survival than the TBI-vehicle group ($p < 0.05$; $p < 0.01$). However, TBI-moderate dose and TBI-high dose groups had no significant differences in the percentage of neuronal survival relative to the sham group ($p > 0.05$) (Figure 4A-C).

Next, we employed glial fibrillary acidic protein (GFAP) to label astrocytes and gauge the amount of reactive gliosis occurring in the brain at 90 days after TBI. Again, no significant differences ($p > 0.05$) were found between groups that received high and moderate doses of stem cells (Figure 5A-C). Moreover, we discovered significantly lower GFAP labeling intensity ($p < 0.05$) in moderate-dose and high-dose groups relative to vehicle and low-dose groups in all brain areas examined (Figure 5A-C). While the vehicle ($p < 0.01$) and low-dose ($p < 0.05$) groups had significantly higher GFAP labeling

intensity than the sham group, there were no significant differences between the sham and moderate-dose, and sham and high-dose groups ($p > 0.05$) (Figure 5A-C).

Labeling for nestin, doublecortin (DCX), and microtubule-associated protein 2 (MAP2) enabled quantification of the expression of phenotypic markers associated with the neural lineage. Immature neurons were labeled with nestin, developing and migrating neurons were labeled with DCX, and mature neurons were labeled with MAP2. At 90 days following TBI, no significant differences were revealed between the high-dose and moderate-dose groups ($p > 0.05$) and between vehicle and low-dose groups ($p > 0.05$) for all brain domains tested and for all nestin, DCX, and MAP2 labeling treatments (Figure 6A-I). Furthermore, transplanting high and moderate amounts of stem cells significantly escalated nestin, DCX, and MAP2 labeling intensity ($p < 0.05$) relative to vehicle and low-dose groups (Figure 6A-H). The vehicle ($p < 0.01$; $p < 0.001$) and low-dose ($p < 0.05$; $p < 0.01$; $p < 0.001$) groups had significantly lower nestin, DCX, and MAP2 labeling intensities than the sham group (Figure 6A-H). While at times the moderate ($p < 0.05$; $p < 0.01$; $p < 0.001$) (Figure 6C, E, H), and high-dose ($p < 0.05$; $p < 0.01$; $p < 0.001$) (Figure 6C, H) groups had significantly lower labeling intensities than the sham group, there were several instances in which the sham

group was not significantly different ($p>0.05$) from the moderate-dose (Figure 6A-B, D, F-G, I) and high-dose (Figure 6A-B, D-G, I) groups.

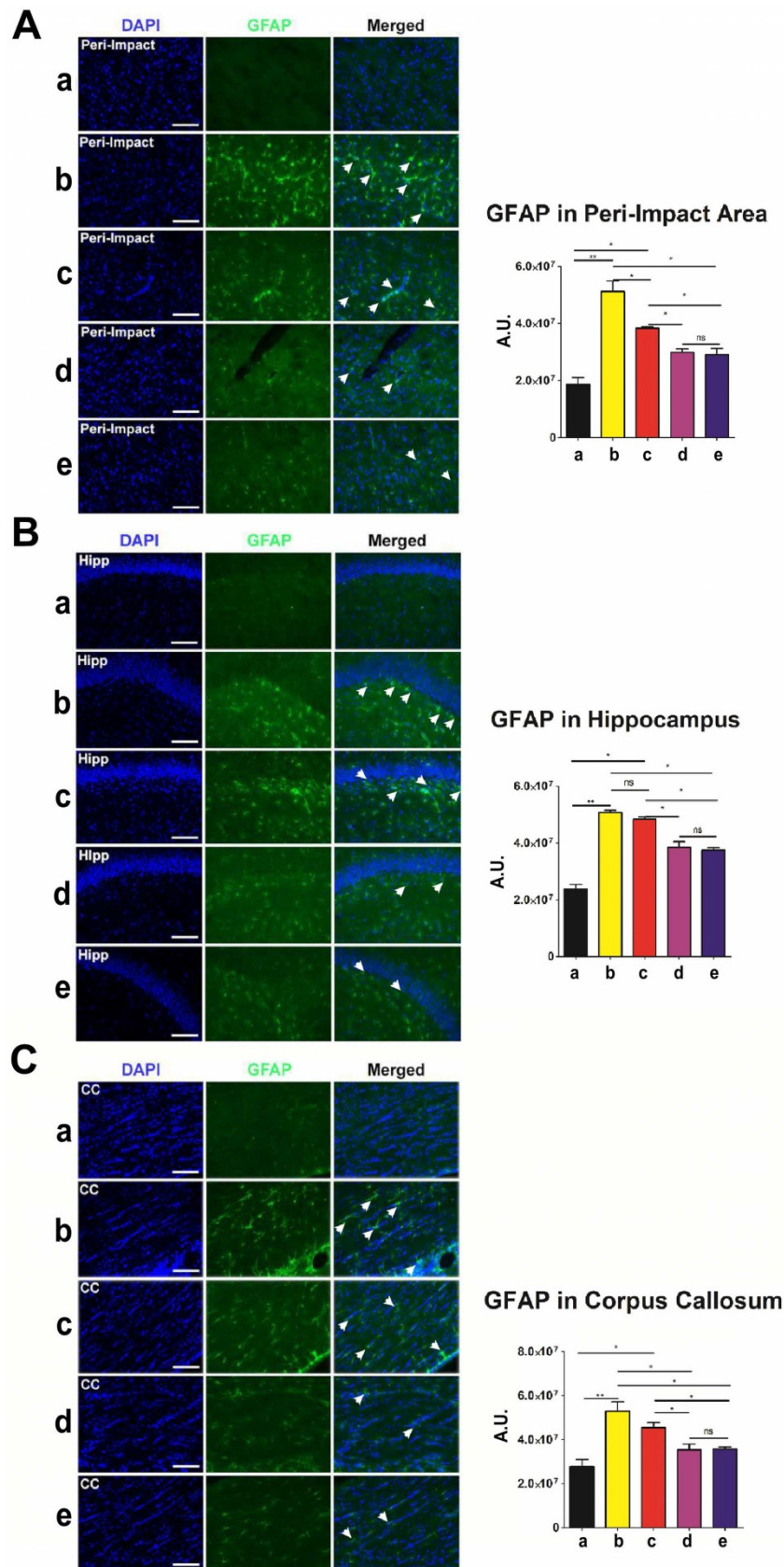


Figure 5. Glial fibrillary acidic protein (GFAP) (green) with DAPI (blue) labeling to assess the occurrence of reactive gliosis in the brain at 90 days post-TBI. Treatment with moderate and high doses of stem cells appeared to reduce reactive gliosis at 90 days post-TBI. Results were analyzed using one-way ANOVA for each

time point (* $p < 0.05$; ** $p < 0.01$; ns $p > 0.05$). ANOVA revealed significant treatment effects. $n = 12$ animals for each group. Arrow heads indicate GFAP-positive cells. Scale bar = 50 μm . a: Sham-Control; b: TBI-Vehicle; c: TBI-Low dose; d: TBI-Moderate dose; e: TBI-High dose; A.U.: average labeling intensity in arbitrary units; Hipp: hippocampus; CC: corpus callosum. **(A)** GFAP immunofluorescence images and quantitative analysis of labeling intensity in the peri-impact area. Statistical analysis: ANOVA ($F(4,15)=28.22$, $p < 0.0001$, Bonferonni's test $p < 0.05$). **(B)** GFAP immunofluorescence images and quantitative analysis of labeling intensity in the hippocampus. Statistical analysis: ANOVA ($F(4,15)=68.28$, $p < 0.0001$, Bonferonni's test $p < 0.05$). **(C)** GFAP immunofluorescence images and quantitative analysis of labeling intensity in the corpus callosum. Statistical analysis: ANOVA ($F(4,15)=11.63$, $p < 0.0001$, Bonferonni's test $p < 0.05$).

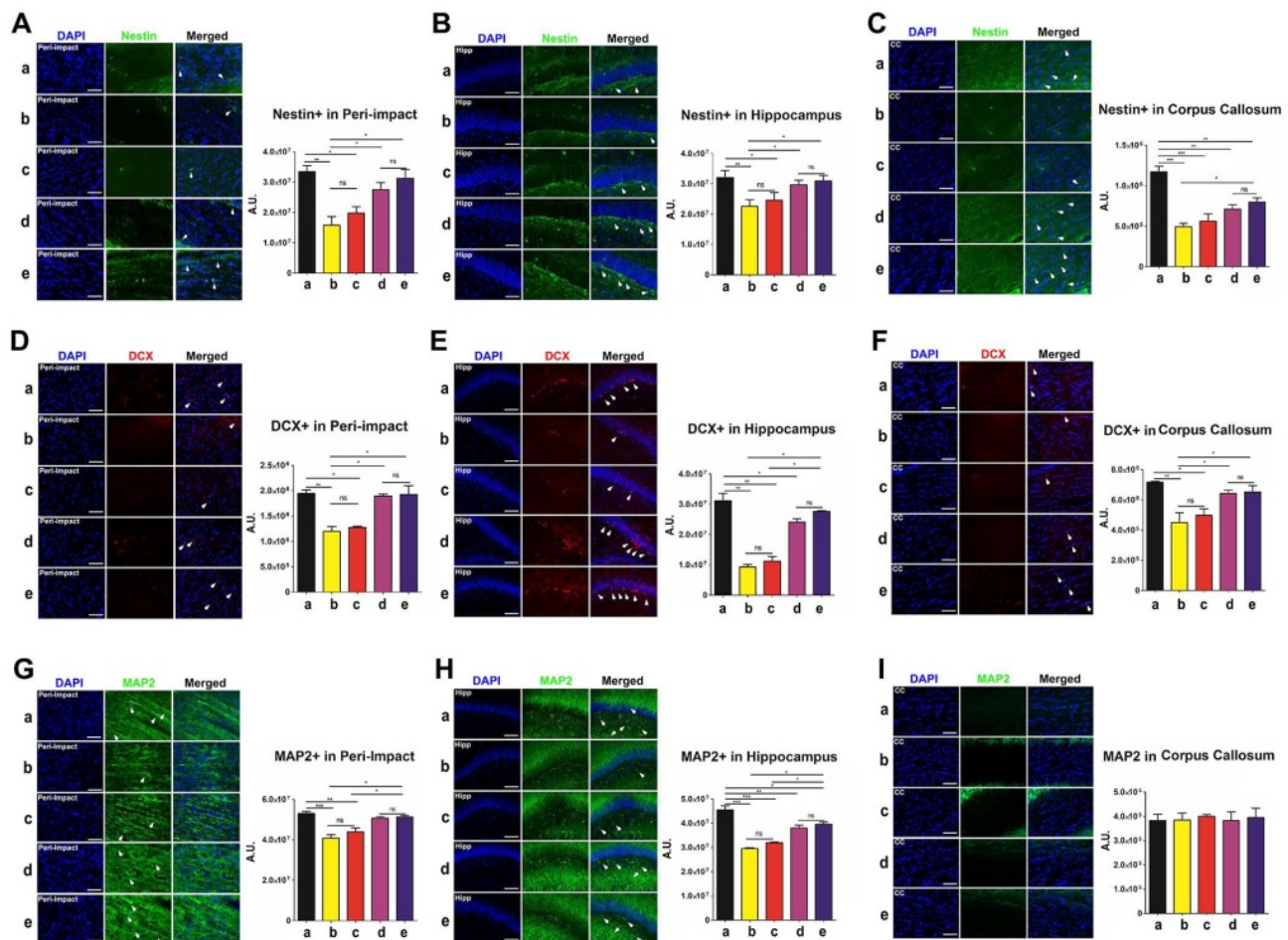


Figure 6. Nestin (green), doublecortin (DCX) (red), and microtubule-associated protein 2 (MAP2) (green) with DAPI (blue) labeling to assess the expression of phenotypic markers related to the neural lineage in the brain at 90 days post-TBI. Treatment with moderate and high doses of stem cells appeared to increase the expression of phenotypic markers associated with the neural lineage at 90 days post-TBI. Results were analyzed using one-way ANOVA for each time point (* $p < 0.05$; ** $p < 0.01$; *** $p < 0.001$; ns $p > 0.05$). $n = 12$ animals for each group. Arrow heads indicate nestin-, DCX-, or MAP2-positive cells. Scale bar = 50 μm . a: Sham-Control; b: TBI-Vehicle; c: TBI-Low dose; d: TBI-Moderate dose; e: TBI-High dose; A.U.: average labeling intensity in arbitrary units; Hipp: hippocampus; CC: corpus callosum. **(A)** Nestin immunofluorescence images and quantitative analysis of labeling intensity in the peri-impact area. Statistical analysis: ANOVA ($F(4,15)=9.377$, $p < 0.0001$, Bonferonni's test $p < 0.05$). **(B)** Nestin immunofluorescence images and quantitative analysis of labeling intensity in the hippocampus. Statistical analysis: ANOVA ($F(4,15)=3.97$, $p < 0.0001$, Bonferonni's test $p < 0.05$). **(C)** Nestin immunofluorescence images and quantitative analysis of labeling intensity in the corpus callosum. Statistical analysis: ANOVA ($F(4,15)=17.65$, $p < 0.0001$, Bonferonni's test $p < 0.05$). **(D)** DCX immunofluorescence images and quantitative analysis of labeling intensity in the peri-impact area. Statistical analysis: ANOVA ($F(4,15)=15.76$, $p < 0.0001$, Bonferonni's test $p < 0.05$). **(E)** DCX immunofluorescence images and quantitative analysis of labeling intensity in the hippocampus. Statistical analysis: ANOVA ($F(4,15)=44.67$, $p < 0.0001$, Bonferonni's test $p < 0.05$). **(F)** DCX immunofluorescence images and quantitative analysis of labeling intensity in the corpus callosum. Statistical analysis: ANOVA ($F(4,15)=7.728$, $p < 0.0001$, Bonferonni's test $p < 0.05$). **(G)** MAP2 immunofluorescence images and quantitative analysis of labeling intensity in the peri-impact area. Statistical analysis: ANOVA ($F(4,15)=14.08$, $p < 0.0001$, Bonferonni's test $p < 0.05$). **(H)** MAP2 immunofluorescence images and quantitative analysis of labeling intensity in the hippocampus. Statistical analysis: ANOVA ($F(4,15)=34.77$, $p < 0.0001$, Bonferonni's test $p < 0.05$). **(I)** MAP2 immunofluorescence images and quantitative analysis of labeling intensity in the corpus callosum. No significant differences were found between all groups ($p > 0.05$).

Next, we labeled myelinated neurons with myelin basic protein (MBP) to investigate myelin expression in the brain at 90 days post-TBI. There were no significant differences in MBP labeling intensity and corpus callosum thickness between the high-dose and moderate-dose groups ($p > 0.05$) and between vehicle and low-dose groups ($p > 0.05$) (Figure 7A-C). We observed significantly more MBP ($p < 0.05$) and a significantly thicker corpus callosum ($p < 0.05$) in the brains of the high-dose group than in the brains of

the vehicle and low-dose groups (Figure 7A-C). The vehicle ($p < 0.05$; $p < 0.001$) and low-dose ($p < 0.05$; $p < 0.01$) groups had a significantly lower MBP labeling intensity and thinner corpus callosus than the sham group (Figure 7A-C). Additionally, the moderate-dose group had significantly thinner corpus callosus than the sham group ($p < 0.05$) (Figure 7C). Furthermore, no significant differences were found between the high-dose and sham groups ($p > 0.05$) (Figure 7A-C).

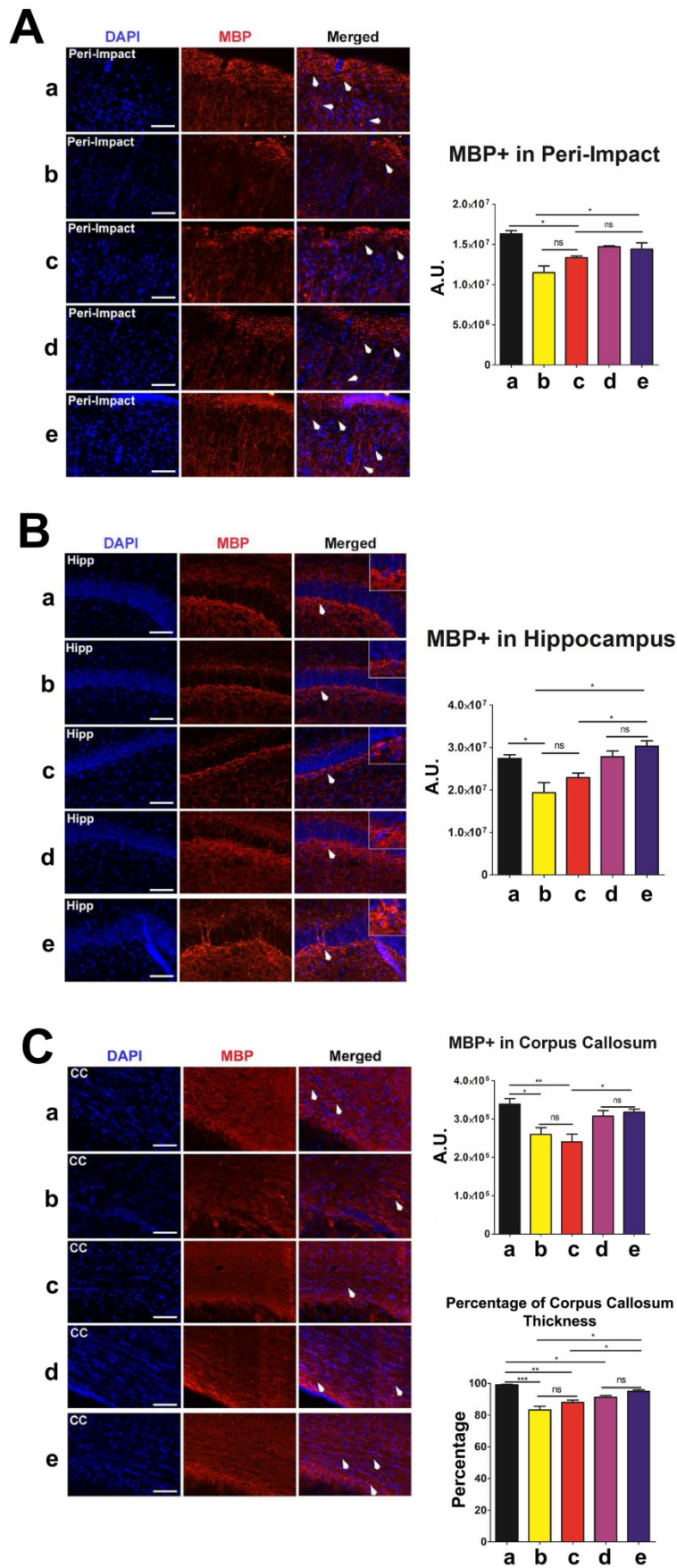


Figure 7. Myelin basic protein (MBP) (red) with DAPI (blue) labeling to assess myelin expression levels in the brain at 90 days post-TBI. Treatment with stem cells, especially high doses, enhanced myelin expression at 90 days post-TBI. Results were analyzed using one-way ANOVA for each time point (* $p < 0.05$; ** $p < 0.01$; *** $p < 0.001$; ns $p > 0.05$). $n = 12$ animals for each group. Arrow heads indicate MBP-positive cells. Scale bar = 50 μm . a: Sham-Control; b: TBI-Vehicle; c: TBI-Low dose; d: TBI-Moderate dose; e: TBI-High dose.

e: TBI-High dose; A.U.: average labeling intensity in arbitrary units; Percentage: corpus callosum thickness of each experimental group expressed as a percentage of the corpus callosum thickness of the sham group; Hipp: hippocampus; CC: corpus callosum. **(A)** MBP immunofluorescence images and quantitative analysis of labeling intensity in the peri-impact area. Statistical analysis: ANOVA revealed significant treatment effects ($F(4,15)=10.70$, $p<0.0001$, Bonferonni's test $p<0.05$). **(B)** MBP immunofluorescence images and quantitative analysis of labeling intensity in the hippocampus. Statistical analysis: ANOVA revealed significant treatment effects ($F(4,15)=8.809$, $p<0.0001$, Bonferonni's test $p<0.05$). **(C)** MBP immunofluorescence images and quantitative analysis of labeling intensity in the corpus callosum and the corpus callosum thickness of each experimental group. Statistical analysis for intensity in the corpus callosum: ANOVA revealed significant treatment effects ($F(4,15)=7.127$, $p<0.0001$, Bonferonni's test $p<0.05$). The corpus callosum thickness of each experimental group was expressed as a percentage of the corpus callosum thickness of the sham group. The high dose treatment group had a significantly thicker corpus callosum relative to those of the vehicle and low dose groups. Statistical analysis for percentage of corpus callosum thickness: ANOVA revealed significant treatment effects ($F(4,15)=18.98$, $p<0.0001$, Bonferonni's test $p<0.05$).

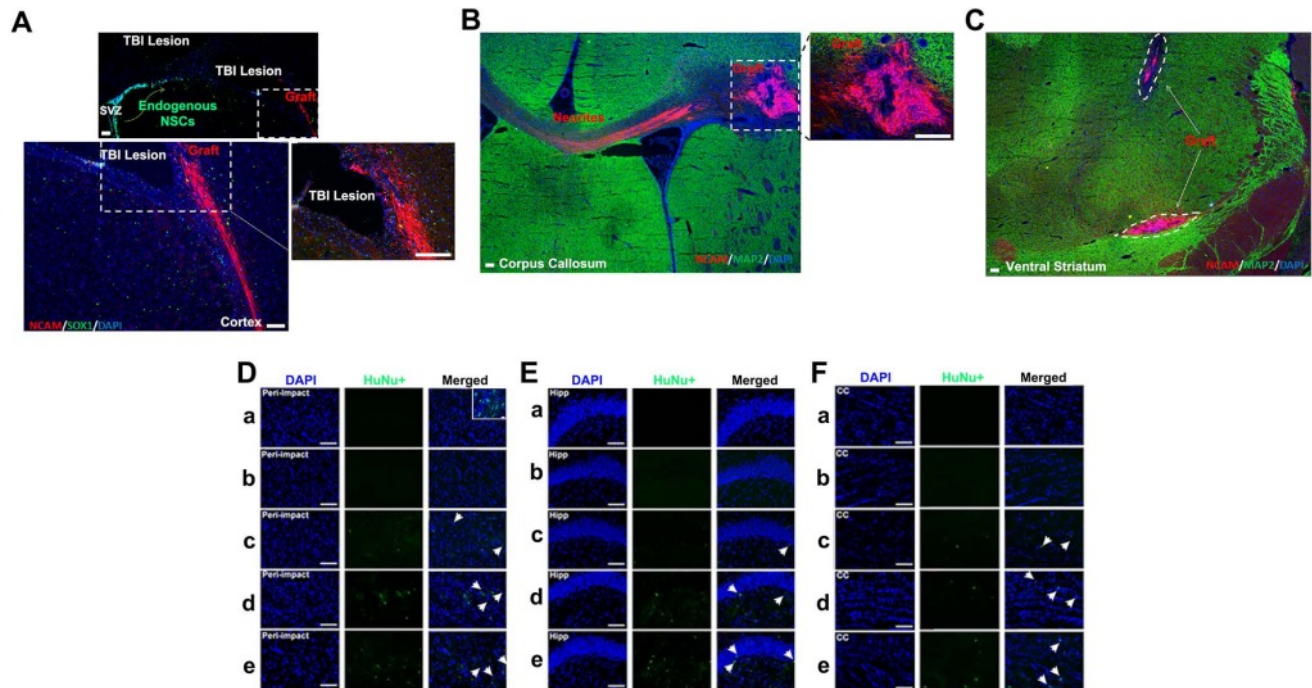


Figure 8. Visualization of transplanted grafts. (A-C) $n = 10$ animals for each group. Animals were perfused on day 17 after TBI. (D-F) $n = 12$ animals for each group. Animals were perfused on day 90 after TBI. **(A)** Neural cell adhesion molecule (NCAM) antibody (ERIC 1) is a mouse monoclonal that detects NCAM of human origin and is non-cross-reactive with NCAM of mouse or rat origin. Portions of the grafts that have committed to the neural lineage are positive for human-specific immature neural marker NCAM. SOX1 antibody detected both human and rat endogenous neural stem cells, some of which migrated from the subventricular zone (SVZ) to the peri-impact lesioned area of the cortex associated with the TBI insult. Scale bar = 200 μm . **(B)** Portions of the grafts that have committed to the neural lineage are positive for human-specific immature neural marker NCAM. MAP2 antibody detects both human and mouse mature neurons. Scale bar = 200 μm . **(C)** Grafts are positive for human-specific immature neural marker NCAM but are negative for mature neuronal marker MAP2. Scale bar = 200 μm . **(D-F)** Human nuclei (HuNu) (green) with DAPI (blue) labeling to determine stem cell graft survival and myelin expression in the brain at 90 days post-TBI. HuNu-positive cells were observed for all stem cell treatment doses and for all brain regions analyzed. Scale bar = 50 μm . Magnification: 20 \times . a: Sham-Control; b: TBI-Vehicle; c: TBI-Low dose; d: TBI-Moderate dose; e: TBI-High dose. Arrow heads indicate HuNu-positive cells. HuNu labeling in the peri-impact area **(D)**, hippocampus (Hipp) **(E)**, and corpus callosum (CC) **(F)** at 90 days post-TBI. **(D)** The small box is a separate image that demonstrates HuNu-positive cells in the peri-impact area at day 10 after TBI. Scale bar = 50 μm .

Neural cell adhesion molecule (NCAM) was employed as a human-specific immature neural marker to identify graft viability during the initial weeks following stem cell transplantation. ISC-hpNSC originally transplanted in the cortex and hippocampus were found in the ventral striatum, suggesting cell migration (**Figure 8C**). To determine how well transplanted ISC-hpNSC survived in the traumatically injured rat brain after an extended period of time, we utilized human nuclei (HuNu) labeling. We detected that while high-dose, moderate-dose, and low-dose groups displayed good graft survival at two weeks post-transplantation as demonstrated by NCAM labeling (**Figure 8A-C**), there was minimal HuNu labeling intensity at 90 days after TBI in all brain zones inspected (**Figure 8D-F**). However, there were HuNu-positive cells in the peri-impact area at day 10 after TBI, as indicated by

the small box in **Figure 8D**.

ISC-hpNSC reduce inflammation as a mechanism to ameliorate TBI

To measure inflammation in the brain and spleen of post-TBI and post-transplant rats, we labeled brain tissues to investigate major histocompatibility complex class II (MHCII) and tumor necrosis factor (TNF) levels, and spleen tissues to investigate OX6 and TNF levels. MHCII and OX6 labeled dendritic cells and microglia and TNF labeled both neurons and splenocytes undergoing inflammatory processes. Organs were harvested, labeled, and analyzed at 90 days post-TBI. There were no statistically significant differences ($p>0.05$) in MHCII and TNF labeling intensity between the high-dose and moderate-dose groups for all brain regions analyzed (**Figure 9A-C**). Additionally,

high-dose and moderate-dose groups produced significantly less labeling intensity ($p < 0.05$) than vehicle and low-dose groups did (Figure 9A-C). The MHCII and TNF labeling intensities in the vehicle ($p < 0.05$; $p < 0.01$; $p < 0.001$) and low-dose ($p < 0.05$; $p < 0.01$)

groups were significantly greater than those in the sham group. No significant differences were observed between the sham and moderate-dose, and between the sham and high-dose groups ($p > 0.05$) (Figure 9A-C).

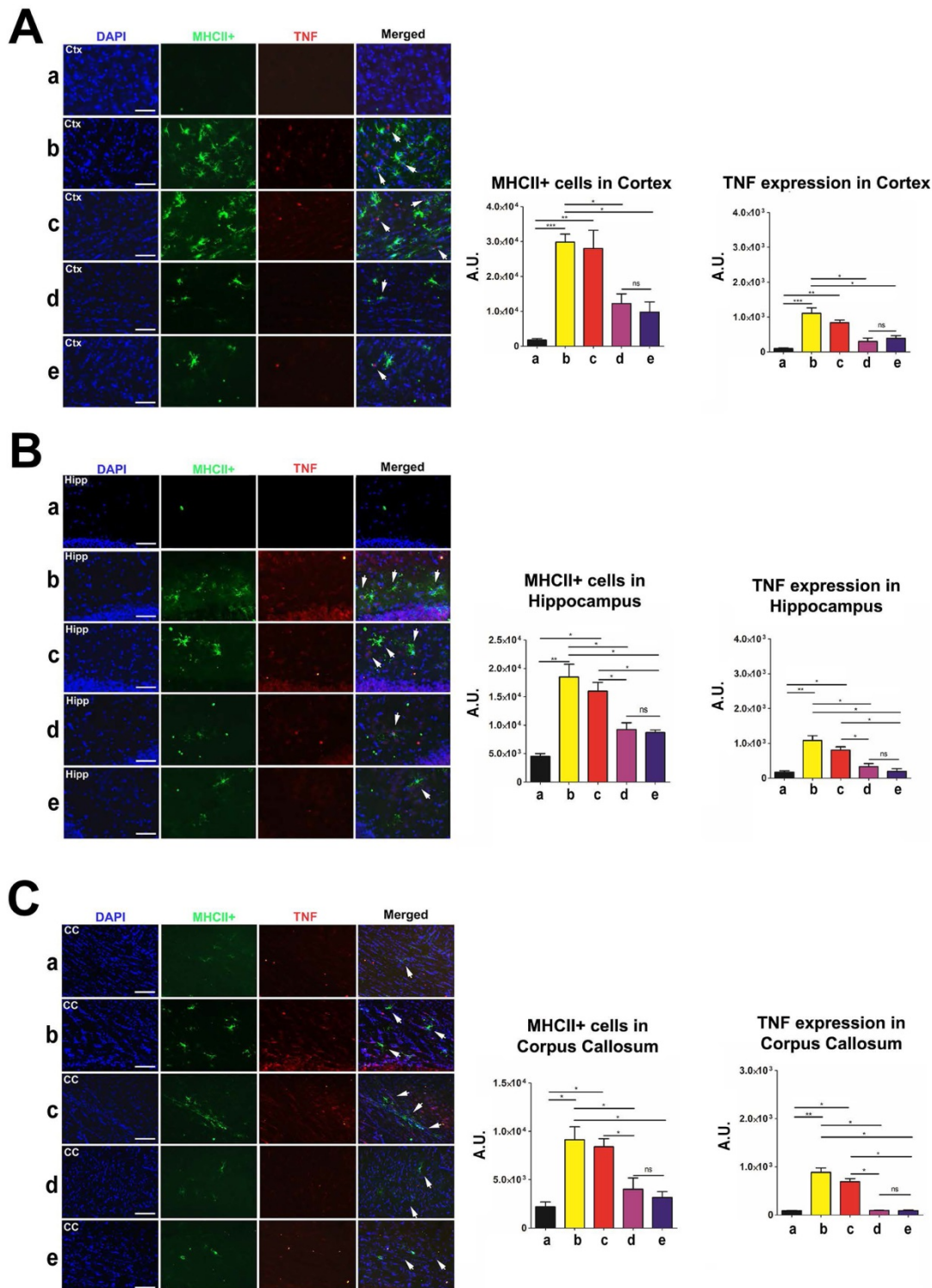


Figure 9. Labeling to determine major histocompatibility complex class II (MHCII) and tumor necrosis factor (TNF) levels in the brain at 90 days post-TBI. Treatment with moderate and high doses of stem cells appeared to modulate the exacerbated inflammatory response and downregulate MHCII and TNF expressions in the brain 90 days post-TBI. Results were analyzed using one-way ANOVA for each time point (* $p < 0.05$; ** $p < 0.01$; *** $p < 0.001$; ns $p > 0.05$). Arrow heads indicate colocalization of MHCII- and TNF-positive cells. $n = 12$ animals for each group. Scale bar = 50 μm . a: Sham-Control; b: TBI-Vehicle; c: TBI-Low dose; d: TBI-Moderate dose; e: TBI-High dose; A.U.: average labeling intensity in arbitrary units; Ctx: cortex; Hipp: hippocampus; CC: corpus callosum. (A) MHCII and TNF immunofluorescence images and quantitative analysis of labeling intensity in the cortex. Statistical analysis for MHCII labeling intensity: ANOVA revealed significant treatment effects ($F(4,15)=15.18$, $p < 0.0001$, Bonferonni's

test $p < 0.05$). Statistical analysis for TNF labeling intensity: ANOVA revealed significant treatment effects ($F(4,15)=19.34$, $p < 0.0001$, Bonferroni's test $p < 0.05$). (B) MHCII and TNF immunofluorescence images and quantitative analysis of labeling intensity in the hippocampus. Statistical analysis for MHCII labeling intensity: ANOVA revealed significant treatment effects ($F(4,15)=17.74$, $p < 0.0001$, Bonferroni's test $p < 0.05$). Statistical analysis for TNF labeling intensity: ANOVA revealed significant treatment effects ($F(4,15)=19.89$, $p < 0.0001$, Bonferroni's test $p < 0.05$). (C) MHCII and TNF immunofluorescence images and quantitative analysis of labeling intensity in the corpus callosum. Statistical analysis for MHCII labeling intensity: ANOVA revealed significant treatment effects ($F(4,15)=11.11$, $p < 0.0001$, Bonferroni's test $p < 0.05$). Statistical analysis for TNF labeling intensity: ANOVA revealed significant treatment effects ($F(4,15)=60.94$, $p < 0.0001$, Bonferroni's test $p < 0.05$).

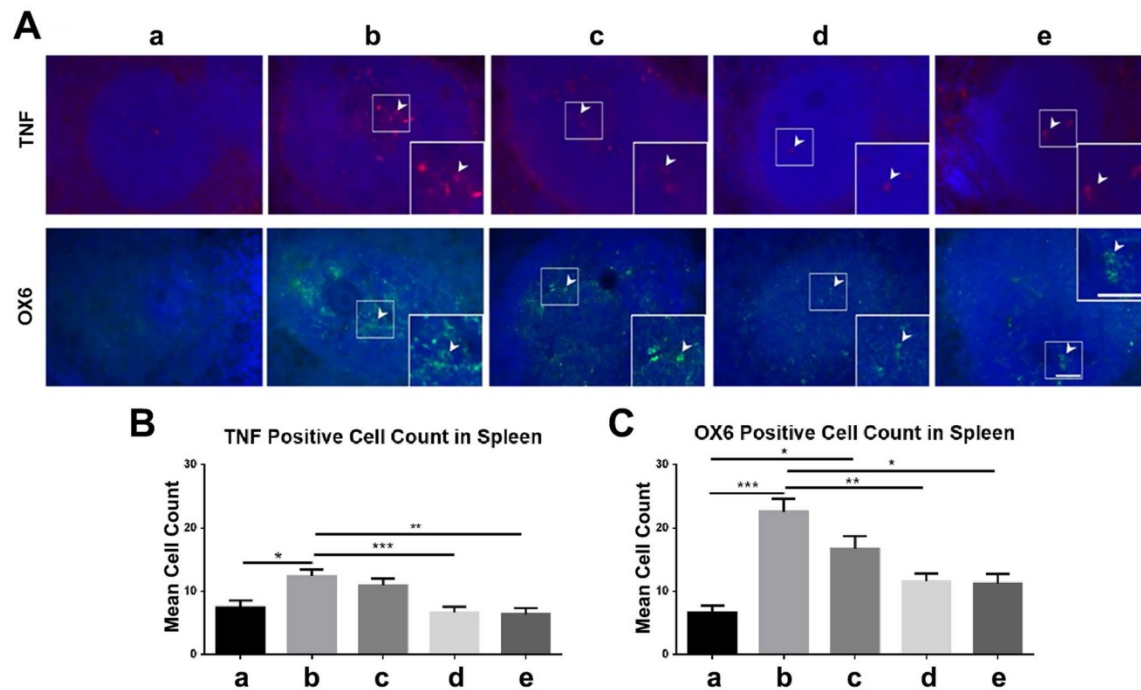


Figure 10. Labeling to evaluate OX6 and tumor necrosis factor (TNF) levels in the spleen at 90 days post-TBI. Treatment with moderate and high doses of stem cells appeared to modulate the exacerbated inflammatory response and downregulate OX6 (green) and TNF (red) expressions in the spleen 90 days post-TBI. $n = 12$ animals for each group. a: sham-control; b: TBI-vehicle; c: TBI-low dose; d: TBI-moderate dose; e: TBI-high dose. (A) Arrow heads indicate TNF-positive and OX6-positive cells. Scale bar = 50 μm . Magnification: 20 \times ; 40 \times (inset). (B) TNF-positive cell count in the spleen. The sham group had significantly fewer TNF-positive cells than the vehicle group ($*p < 0.05$). The moderate and high dose groups had significantly fewer TNF-positive cells than the vehicle group ($***p < 0.01$; $***p < 0.001$). (C) OX6-positive cell count in the spleen. The sham group had significantly fewer OX6-positive cells than the vehicle ($***p < 0.001$) and low dose ($*p < 0.05$) groups. The moderate and high dose groups had significantly fewer OX6-positive cells than the vehicle group ($*p < 0.05$; $**p < 0.01$).

Similarly, there were significantly fewer OX6-positive and TNF-positive cells ($p < 0.05$; $p < 0.01$; $p < 0.001$) in the spleens of high-dose and moderate-dose groups than in the spleens of vehicle and low-dose groups (Figure 10A-C). The vehicle group had significantly more TNF-positive cells than the sham group ($p < 0.05$) (Figure 10B) and the vehicle ($p < 0.001$) and low-dose ($p < 0.05$) groups had significantly more OX6-positive cells than the sham group (Figure 10C). Also, the sham, moderate-dose, and high-dose groups had no significant differences in OX6-positive and TNF-positive cell counts in the spleen (Figure 10A-C).

Discussion

Previous studies show dose-response efficacy readouts for different types of stem cells (e.g., NT2N, Muse cells, Notch-induced BMSCs) with a therapeutic dose range of 40,000 to 200,000 cells [33-36]. Accordingly, in the present study we designated 50,000, 100,000, and 200,000 viable ISC-hpNSC as the low, moderate, and high dose, respectively. In this study, we probed the idea that introducing

ISC-hpNSC grafts intracerebrally at 72 h post-TBI would ameliorate TBI-induced behavioral and histological deficits in pre-clinical TBI model rats. Our results demonstrate that ISC-hpNSC transplants corrected swing biases on the EBST if given at high or moderate doses, suggesting that higher quantities of ISC-hpNSC are necessary to significantly remedy diminished locomotor function. In contrast, stem cell treatment did not increase TBI subjects' time on the rotarod test, indicating that ISC-hpNSC were not successful in restoring motor coordination. For the neurological evaluation, ISC-hpNSC enhanced forelimb akinesia and paw grasp scores for all treatment groups, but the results imply that progressively higher doses correlate with increased recovery of neurological function. TBI rats were still capable of learning and memorization, as all TBI groups had fewer errors with each successive trial on the RAWM test. However, animals given high and moderate doses of ISC-hpNSC made fewer mistakes, suggesting that only larger volumes of stem cell transplants can effectively repair TBI-associated cognitive impairments. Interestingly, since no

significant difference was found between high-dose and moderate-dose groups, it is possible that injecting a specific minimum quantity of ISC-hpNSC is sufficient to achieve similar therapeutic effects on cognition as a higher dose would.

Histological analyses unveiled the outcomes of ISC-hpNSC transplantation on TBI rats at the tissue level at 90 days after injury. In the peri-impact area of the cortex, the TBI-vehicle group had significantly less neuronal survival compared to the sham group, demonstrating that the TBI produced significant cortical damage. In contrast, the quantity of surviving neurons in TBI groups given moderate or high doses of ISC-hpNSC were not significantly different from that of the sham group, indicating that transplanting moderate and high doses of ISC-hpNSC reversed this TBI-induced cortical damage. High and moderate injections of stem cells led to abated MHCII and TNF labeling intensity in the brain and fewer OX6-positive and TNF-positive cells in the spleen, implying reduced inflammation and supporting the idea that the spleen is correlated to inflammation levels in the brain [37, 38]. Similarly, high-dose and moderate-dose groups showed less intense GFAP labeling, indicating decreased reactive gliosis. Additionally, the expression of phenotypic markers related to the neural lineage increased with high and moderate volumes of ISC-hpNSC, as exhibited by intense nestin, DCX, and MAP2 labeling. Moreover, we observed enhanced myelin expression as signified by a higher MBP labeling intensity and a thicker corpus callosum in subjects receiving high doses of stem cells. Finally, a low amount of HuNu labeling in all ISC-hpNSC treatment groups denoted poor long-term graft survival and differentiation. No significant difference was found between high-dose and moderate-dose groups across all labeling experiments, indicating that these doses produce similar levels of histological responses. Furthermore, all brain regions analyzed experienced improved TBI-related deficits, suggesting that ISC-hpNSC effects spread over wide areas and are not confined to a localized space.

Previous studies demonstrated that ISC-hpNSC transplanted into the striatum and substantia nigra mitigate the symptoms of Parkinson's disease (PD) and increase dopamine levels and striatal dopaminergic innervation in non-human primates [13]. The current study advances their use with a new approach—applying ISC-hpNSC intracerebrally to alleviate the detrimental effects of TBI. From the PD monkey and rodent studies, we previously determined that ISC-hpNSC exerted their therapeutic properties by migrating, increasing neurotrophic factors, and upregulating genes that were previously

inhibited by PD in order to increase dopaminergic neuron quantity and innervation [13, 23]. In the PD monkey study at 12 months after injection, we observed that stem cell grafts survived and successfully differentiated into dopaminergic neurons [13]. In a similar way, we believe that the widespread histological improvements in all areas we examined in the current investigation—corpus callosum, hippocampus, striatum, peri-impact area, spleen—indicate a way for transplanted ISC-hpNSC to migrate and treat affected tissues away from the initial injection site. Based on our present results, we propose that ISC-hpNSC protect tissues from TBI-related destruction by reducing inflammation to limit secondary biochemical pathway damage and increasing the expression of phenotypic markers associated with the neural lineage and myelination to promote neuronal health. Since we observed inferior long-term graft survival and differentiation but prolonged improvements at the tissue and behavioral levels, it is likely that transplanted ISC-hpNSC travel to afflicted sectors in the brain and secrete factors, such as anti-inflammatory molecules, to mitigate inflammation-induced damage to neurons. Indeed, our previous investigation with ISC-hpNSC demonstrated that these grafted cells migrate and increase trophic factors in animal models of PD [13, 23] and other research have indicated that stem cells secrete neurotrophic factors to promote the recovery of injured brain tissue [39] and release proteins such as bone morphogenetic protein-4 that influence cell fate [40]. In our present study, this would explain how ISC-hpNSC ameliorates TBI-associated histological deficits and, consequently, behavioral deficits, even as the stem cell grafts disappear.

Using ISC-hpNSC has several advantages over utilizing other types of stem cells for treating TBI. For instance, working with embryonic stem cells raises ethical concerns regarding sacrificing a potential embryo, whereas ISC-hpNSC are generated by chemically activating an unfertilized egg cell [13, 16, 17]. Additionally, ISC-hpNSC are easily obtained and can form a self-propagating, endless source of homogenous stem cells that can be cryopreserved [12-15]. hpSCs derived as homozygous for prevalent human leukocyte antigen types also have the ability to immune match numerous patients which adds to their translatability and utility in the clinic [10, 18-20]. Moreover, our study demonstrated that when ISC-hpNSC were transplanted intracerebrally, the grafts barely survived and differentiated at 90 days after injury, yet TBI-precipitated complications were successfully rehabilitated. Although past studies with ISC-hpNSC exhibited that these cells are unlikely to form tumors or prompt other problems, the transient

nature of the grafts shown in our TBI study would further lessen any detrimental risks connected to stem cell transplantation [10, 13, 23]. Additionally, Johannesson et al. discovered that human nuclear-transfer embryonic stem cells and isogenic induced pluripotent stem cells had a significantly higher incidence of de novo mutations relative to parthenogenetic embryonic stem cells, suggesting that parthenogenetic stem cells like ISC-hpNSC may be less prone to tumor formation than other stem cell variants [41].

The results elicited several questions that were not fully addressed through the present study but could be pursued in future research. For instance, we noted that the stem cell grafts had poor survivability and differentiation, but previous studies suggested that these ISC-hpNSC grafts should have survived for an extended period of time and differentiated into appropriate cells [13]. It is possible that the immunosuppression employed in previous PD studies hinders a host rejection response to the transplanted grafts and the TBI lesion in the present study creates a toxic environment that is less conducive to transplanted stem cell survival [1, 13, 23, 42]. In addition, the results suggest that ISC-hpNSC recover tissues injured from TBI, but the study could not completely explain the mechanism by which stem cells reduce inflammation, reduce reactive gliosis, increase the expression of phenotypic markers related to the neural lineage, and increase myelination. Further investigations would clarify if ISC-hpNSC secrete certain factors like anti-inflammatory molecules as suspected or execute these changes via another method or pathway. While it is interesting to note how ISC-hpNSC administration reduced inflammation in both the brain and the spleen, the mechanism behind these changes in the spleen is still uncertain but is potentially affiliated with the immunity-based connection between the two organs, as discussed in past studies [37, 38]. Also, the current study does not identify why mainly moderate and high doses of stem cells were key to improving TBI-related impairments and why at times moderate doses were as effective as high doses. It is possible that there is a minimum dose of ISC-hpNSC required to exert therapeutic effects and that these effects are not necessarily enhanced by higher doses. In fact, prior stem cell transplant studies have shown that higher transplant doses were correlated with improved neuroprotection [43], cardiac perfusion [44], and immune reconstitution speed [45] compared to low doses, and found no differences in neuroprotective effects between a specific minimum dose volume and higher doses [43]. Ultimately, further studies addressing the limitations of this study

and exploring these unanswered questions would be beneficial for determining the exact mechanisms by which ISC-hpNSC heal tissues.

Overall, high and moderate doses of ISC-hpNSC ameliorated TBI-associated histological alterations and TBI-related motor, neurological, and cognitive deficits. We introduce a novel, potential mechanism in which transplanted ISC-hpNSC migrate to damaged regions and emit factors that reduce inflammation and reactive gliosis and increase the expression of phenotypic markers associated with the neural lineage and myelination. Safety studies of ISC-hpNSC incorporating in vitro and in vivo experiments indicated that the cells were not tumorigenic, possessed inconsequential amounts of undifferentiated human pluripotent stem cells, did not form teratomas, were tolerated well by animals, and displayed no toxicity [10, 23]. Additionally, the monkey PD studies also substantiated ISC-hpNSC safety, as the monkeys injected with ISC-hpNSC handled the cells well, experienced no tumors, formed no ectopic tissue, and did not encounter any other inimical effects [13]. These past results combined with our current study's observation that grafted stem cells had a short lifespan in TBI brains further attest to the safety of administering ISC-hpNSC in the clinic. Moreover, ISC-hpNSC improved disease symptoms in both the past PD studies and our current TBI study, which vouches for ISC-hpNSC efficaciousness in clinical applications [13, 23]. A current Phase I clinical trial (Clinicaltrials.gov identifier NCT02452723) at the Royal Melbourne Hospital in Australia is evaluating the safety of ISC-hpNSC in human PD patients [46]. Positive results from the ongoing PD clinical trial, initiating ISC-hpNSC clinical trials for TBI patients, and additional pre-clinical ISC-hpNSC studies will help translate ISC-hpNSC into clinical cell-based therapies to treat TBI and other neurological diseases.

Abbreviations

ANOVA: analysis of variance; CCI: controlled cortical impact; DCX: doublecortin; EBST: elevated body swing test; GFAP: glial fibrillary acidic protein; hpSCs: human parthenogenetic stem cells; IACUC: Institutional Animal Care and Use Committee; ISCO: International Stem Cell Corporation; IHC: immunohistochemistry; ISC-hpNSC: International Stem Cell Corporation human parthenogenetic neural stem cells; MAP2: microtubule-associated protein 2; MBP: myelin basic protein; MHCII: major histocompatibility complex class II; NCAM: neural cell adhesion molecule; ns: not significant; PD: Parkinson's disease; RAWM: radial arm water maze; TBI: traumatic brain injury; TNF: tumor necrosis factor.

Competing Interests

A.S., I.G., R.G., and R.K. are employees and stock holders of International Stem Cell Corporation. C.V.B. received funding from International Stem Cell Corporation for this study.

References

- Lozano D, Gonzales-Portillo GS, Acosta S, de la Pena I, Tajiri N, Kaneko Y, et al. Neuroinflammatory responses to traumatic brain injury: etiology, clinical consequences, and therapeutic opportunities. *Neuropsychiatr Dis Treat*. 2015; 11: 97-106.
- Tajiri N, Kellogg SL, Shimizu T, Arendash GW, Borlongan CV. Traumatic brain injury precipitates cognitive impairment and extracellular Abeta aggregation in Alzheimer's disease transgenic mice. *PLoS One*. 2013; 8: e78851.
- Acosta SA, Tajiri N, Sanberg PR, Kaneko Y, Borlongan CV. Increased amyloid precursor protein and tau expression manifests as key secondary cell death in chronic traumatic brain injury. *J Cell Physiol*. 2017; 232: 665-77.
- Faul M, Xu L, Wald MM, Coronado VG. Traumatic Brain Injury in the United States: Emergency Department Visits, Hospitalizations, and Deaths. Atlanta, USA: Centers for Disease Control and Prevention, National Center for Injury Prevention and Control; 2010.
- Maas AI, Stocchetti N, Bullock R. Moderate and severe traumatic brain injury in adults. *Lancet Neurol*. 2008; 7: 728-41.
- Werner C, Engelhard K. Pathophysiology of traumatic brain injury. *Br J Anaesth*. 2007; 99: 4-9.
- Shlosberg D, Benifla M, Kaufer D, Friedman A. Blood-brain barrier breakdown as a therapeutic target in traumatic brain injury. *Nat Rev Neurol*. 2010; 6: 393-403.
- Wang GH, Jiang ZL, Li YC, Li X, Shi H, Gao YQ, et al. Free-radical scavenger edaravone treatment confers neuroprotection against traumatic brain injury in rats. *J Neurotrauma*. 2011; 28: 2123-34.
- Acosta SA, Tajiri N, Shinozuka K, Ishikawa H, Sanberg PR, Sanchez-Ramos J, et al. Combination therapy of human umbilical cord blood cells and granulocyte colony stimulating factor reduces histopathological and motor impairments in an experimental model of chronic traumatic brain injury. *PLoS One*. 2014; 9: e90953.
- Garitaonandia I, Gonzalez R, Christiansen-Weber T, Abramihina T, Poustovoitov M, Noskov A, et al. Neural stem cell tumorigenicity and biodistribution assessment for phase I clinical trial in Parkinson's disease. *Sci Rep*. 2016; 6: 34478.
- Ratcliffe E, Glen KE, Naing MW, Williams DJ. Current status and perspectives on stem cell-based therapies undergoing clinical trials for regenerative medicine: case studies. *Br Med Bull*. 2013; 108: 73-94.
- Gonzalez R, Garitaonandia I, Abramihina T, Wambua GK, Ostrowska A, Brock M, et al. Deriving dopaminergic neurons for clinical use. A practical approach. *Sci Rep*. 2013; 3: 1463.
- Gonzalez R, Garitaonandia I, Poustovoitov M, Abramihina T, McEntire C, Culp B, et al. Neural stem cells derived from human parthenogenetic stem cells engraft and promote recovery in a nonhuman primate model of Parkinson's disease. *Cell Transplant*. 2016; 25: 1945-66.
- Isaev DA, Garitaonandia I, Abramihina TV, Zogovic-Kapsalis T, West RA, Semechkin AY, et al. In vitro differentiation of human parthenogenetic stem cells into neural lineages. *Regen Med*. 2012; 7: 37-45.
- Revazova ES, Turovets NA, Kochetkova OD, Kindarova LB, Kuzmichev LN, Janus JD, et al. Patient-specific stem cell lines derived from human parthenogenetic blastocysts. *Cloning Stem Cells*. 2007; 9: 432-49.
- Lo B, Parham L. Ethical issues in stem cell research. *Endocr Rev*. 2009; 30: 204-13.
- Turovets N, Fair J, West R, Ostrowska A, Semechkin R, Janus J, et al. Derivation of high-purity definitive endoderm from human parthenogenetic stem cells using an in vitro analog of the primitive streak. *Cell Transplant*. 2012; 21: 217-34.
- Daughtry B, Mitalipov S. Concise review: parthenote stem cells for regenerative medicine: genetic, epigenetic, and developmental features. *Stem Cells Transl Med*. 2014; 3: 290-8.
- Revazova ES, Turovets NA, Kochetkova OD, Agapova LS, Sebastian JL, Pryzhkova MV, et al. HLA homozygous stem cell lines derived from human parthenogenetic blastocysts. *Cloning Stem Cells*. 2008; 10: 11-24.
- Taylor CJ, Bolton EM, Pocock S, Sharples LD, Pedersen RA, Bradley JA. Banking on human embryonic stem cells: estimating the number of donor cell lines needed for HLA matching. *Lancet*. 2005; 366: 2019-25.
- Carpenter MK, Frey-Vasconcells J, Rao MS. Developing safe therapies from human pluripotent stem cells. *Nat Biotechnol*. 2009; 27: 606-13.
- Frey-Vasconcells J, Whittlesey KJ, Baum E, Feigl EG. Translation of stem cell research: points to consider in designing preclinical animal studies. *Stem Cells Transl Med*. 2012; 1: 353-8.
- Gonzalez R, Garitaonandia I, Crain A, Poustovoitov M, Abramihina T, Noskov A, et al. Proof of concept studies exploring the safety and functional activity of human parthenogenetic-derived neural stem cells for the treatment of Parkinson's disease. *Cell Transplant*. 2015; 24: 681-90.
- Acosta SA, Tajiri N, Hoover J, Kaneko Y, Borlongan CV. Intravenous bone marrow stem cell grafts preferentially migrate to spleen and abrogate chronic inflammation in stroke. *Stroke*. 2015; 46: 2616-27.
- Boutajangout A, Noorwali A, Atta H, Wisniewski T. Human umbilical cord stem cell xenografts improve cognitive decline and reduce the amyloid burden in a mouse model of Alzheimer's disease. *Curr Alzheimer Res*. 2017; 14: 104-11.
- Garbuzova-Davis S, Kurien C, Thomson A, Falco D, Ahmad S, Staffetti J, et al. Endothelial and astrocytic support by human bone marrow stem cell grafts into symptomatic ALS mice towards blood-spinal cord barrier repair. *Sci Rep*. 2017; 7: 884.
- Tajiri N, Acosta SA, Shahaduzzaman M, Ishikawa H, Shinozuka K, Pabon M, et al. Intravenous transplants of human adipose-derived stem cell protect the brain from traumatic brain injury-induced neurodegeneration and motor and cognitive impairments: cell graft biodistribution and soluble factors in young and aged rats. *J Neurosci*. 2014; 34: 313-26.
- Tajiri N, Duncan K, Antoine A, Pabon M, Acosta SA, de la Pena I, et al. Stem cell-paved biobridge facilitates neural repair in traumatic brain injury. *Front Syst Neurosci*. 2014; 8: 116.
- Paxinos G, Watson C. *The Rat Brain in Stereotaxic Coordinates*. 2nd ed. San Diego, USA: Academic Press; 1986.
- Borlongan CV, Sanberg PR. Elevated body swing test: a new behavioral parameter for rats with 6-hydroxydopamine-induced hemiparkinsonism. *J Neurosci*. 1995; 15: 5372-8.
- Altumbabic M, Peeling J, Del Bigio MR. Intracerebral hemorrhage in the rat: effects of hematoma aspiration. *Stroke*. 1998; 29: 1917-22; discussion 22-3.
- Yasuhara T, Hara K, Maki M, Mays RW, Deans RJ, Hess DC, et al. Intravenous grafts recapitulate the neurorestoration afforded by intracerebrally delivered multipotent adult progenitor cells in neonatal hypoxic-ischemic rats. *J Cereb Blood Flow Metab*. 2008; 28: 1804-10.
- Yasuhara T, Matsukawa N, Hara K, Maki M, Ali MM, Yu SJ, et al. Notch-induced rat and human bone marrow stromal cell grafts reduce ischemic cell loss and ameliorate behavioral deficits in chronic stroke animals. *Stem Cells Dev*. 2009; 18: 1501-14.
- Uchida H, Niizuma K, Kushida Y, Wakao S, Tominaga T, Borlongan CV, et al. Human Muse cells reconstruct neuronal circuitry in subacute lacunar stroke model. *Stroke*. 2017; 48: 428-35.
- Borlongan CV, Tajima Y, Trojanowski JQ, Lee VM, Sanberg PR. Transplantation of cryopreserved human embryonic carcinoma-derived neurons (NT2N cells) promotes functional recovery in ischemic rats. *Exp Neurol*. 1998; 149: 310-21.
- Saporta S, Borlongan CV, Sanberg PR. Neural transplantation of human neuroteratocarcinoma (hNT) neurons into ischemic rats. A quantitative dose-response analysis of cell survival and behavioral recovery. *Neuroscience*. 1999; 91: 519-25.
- Ajmo CT, Jr., Vernon DO, Collier L, Hall AA, Garbuzova-Davis S, Willing A, et al. The spleen contributes to stroke-induced neurodegeneration. *J Neurosci Res*. 2008; 86: 2227-34.
- Li M, Li F, Luo C, Shan Y, Zhang L, Qian Z, et al. Immediate splenectomy decreases mortality and improves cognitive function of rats after severe traumatic brain injury. *J Trauma*. 2011; 71: 141-7.
- Chen Q, Long Y, Yuan X, Zou L, Sun J, Chen S, et al. Protective effects of bone marrow stromal cell transplantation in injured rodent brain: synthesis of neurotrophic factors. *J Neurosci Res*. 2005; 80: 611-9.
- Wislet-Gendebien S, Bruyere F, Hans G, LePrince P, Moonen G, Rogister B. Nestin-positive mesenchymal stem cells favour the astroglial lineage in neural progenitors and stem cells by releasing active BMP4. *BMC Neurosci*. 2004; 5: 33.
- Johannesson B, Sagi I, Gore A, Paull D, Yamada M, Golan-Lev T, et al. Comparable frequencies of coding mutations and loss of imprinting in human pluripotent cells derived by nuclear transfer and defined factors. *Cell Stem Cell*. 2014; 15: 634-42.
- Wood KJ, Bushell A, Hester J. Regulatory immune cells in transplantation. *Nat Rev Immunol*. 2012; 12: 417-30.
- Robinson AM, Rahman AA, Miller S, Stavely R, Sakkal S, Nurgali K. The neuroprotective effects of human bone marrow mesenchymal stem cells are dose-dependent in TNBS colitis. *Stem Cell Res Ther*. 2017; 8: 87.

44. Quyyumi AA, Waller EK, Murrow J, Esteves F, Galt J, Oshinski J, et al. CD34(+) cell infusion after ST elevation myocardial infarction is associated with improved perfusion and is dose dependent. *Am Heart J.* 2011; 161: 98-105.
45. Chen BJ, Cui X, Sempowski GD, Domen J, Chao NJ. Hematopoietic stem cell dose correlates with the speed of immune reconstitution after stem cell transplantation. *Blood.* 2004; 103: 4344-52.
46. Garitaonandia I, Gonzalez R, Sherman G, Semechkin A, Evans A, Kern R. Novel approach to stem cell therapy in Parkinson's disease. *Stem Cells Dev.* 2018; 27: 951-7.